Altair® FluxMotor® 2026

Reluctance Synchronous Machines - Inner rotor

Motor Factory - Test - Characterization

General user information

Contents

CHARACTERIZATION – MODEL – MOTOR – MAPS

1.1 Positioning and objective

The aim of the test “Characterization - Model - Motor - Maps” is to give 2D maps in J_d-J_q plane for characterizing the 3-Phase reluctance synchronous machines.

These maps allow predicting the behavior of the electrical rotating machine at a system level.

In this test engineers will find a system integrator and / or control-command tool adapted to their needs and able to provide accurate maps ready to be used in system simulation software like Activate.

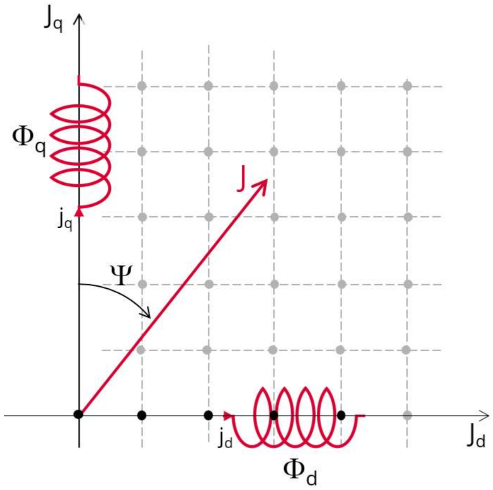

“Characterization - Model - Motor - Maps” illustration

Performance of the machine in steady state can be deduced from the results obtained in this test in association with the drive and control mode to be considered.

The following table helps to classify the test:

Family	Characterization
Package	Model
Convention	Motor
Test	Maps

Positioning of the test “Characterization - Model - Motor - Maps”

1.2 Main principles of computation

1.2.1 Flux linkage

One of the goals is to compute the D-axis and Q-axis flux linkage in the J_d, J_q plane.
To do that, a grid of values (J_d, J_q) is considered.
For each node of this grid, the corresponding flux linkage through each phase is extracted (Φ_a, Φ_b, Φ_c) through corresponding phases a, b, c). This is done using Finite Element modelling (Flux® software – Magnetostatic application).
D-axis flux-linkage component - Φ_d and **Q-axis flux-linkage component -** Φ_q are deduced according to Park's transformation.

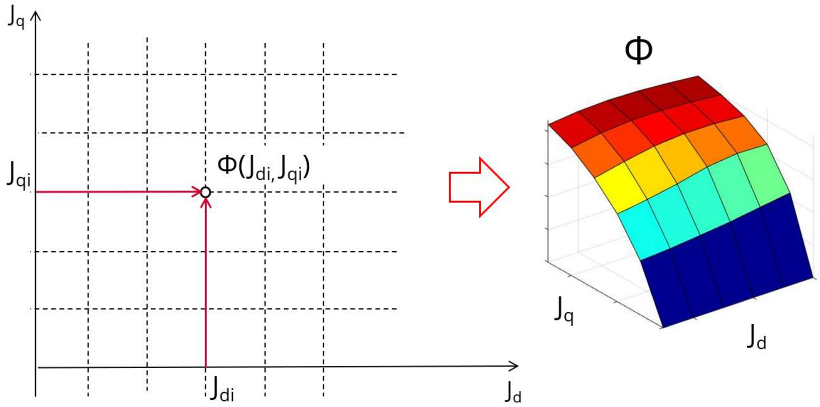

Computation on a grid in J_d, J_q plane

Our modeling considers cross-saturation. However, neither winding harmonics nor the variation of reluctance as a function of angular position of the rotor are considered.

Note: The impact on accuracy will be more important for machine with high level of saturation.
Iron loss computations are based on both a Finite Element modelling and on an analytical method where leakage flux between stator teeth is neglected.
In case of high level of saturation, this hypothesis leads to more errors particularly in the area where there is field weakening.

Note: In the examples shown in the images, positive value of J_d and positive value of J_q are considered. These values ranges correspond to the working conditions for a motor. However, the considered quadrants can be chosen through dedicated input (e.g., user can choose all quadrants, or only the 2nd, the 2nd and 3rd one, etc.) allowing the characterization of the machine behavior for other control conditions.

Note: In case the Rotor position dependency is set to "Yes", the computation is done in the J_d - J_q plane with an additional third axis corresponding to the rotor position θ_r.

1.2.2 Flux-linkage derivative respect to the rotor position

D-axis flux-linkage derivative with respect to the rotor position - $\Phi_d/d\theta_r$ and **Q-axis flux-linkage derivative with respect to the rotor position -** $\Phi_q/d\theta_r$ are computed from the flux linkage maps and using the following formulae:

$$\frac{\Delta\Phi_d}{\Delta\theta_r} \qquad \frac{\Delta\Phi_q}{\Delta\theta_r}$$

These maps are available only when the input Rotor position dependency is set to "Yes". The computation is done in the J_d - J_q plane with an additional third axis corresponding to the rotor position θ_r.

Note 1: The rotor position derivative is always in radians per second to simplify the usage of this map while considering the Park's voltage equations.

1.2.3 Dynamic inductances

D-axis synchronous inductance - $L_{d-dynamic}$ and **Q-axis synchronous inductance - $L_{q-dynamic}$** are computed from the flux linkage maps and using the following formulae:

$$L_{d-dynamic} = \frac{\Delta\Phi_d}{\Delta J_d} \qquad L_{q-dynamic} = \frac{\Delta\Phi_q}{\Delta J_q}$$

Note 1: The end-winding leakage inductance L_{endw}, computed in the winding area, is included in the computation of D-axis and Q-axis flux-linkage. The values of the dynamic inductances $L_{d-dynamic}$ and $L_{q-dynamic}$ consider the value of the end-winding inductance.

Note 2: In the previous formulae, one considers peak values for both flux and current.

Note 3: In case the Rotor position dependency is set to "Yes", the computation is done in the J_d - J_q plane with an additional third axis corresponding to the rotor position θ_r.

1.2.4 Dynamic cross inductances

D-axis synchronous cross inductance - $L_{dq-dynamic}$ and **Q-axis synchronous cross inductance - $L_{qd-dynamic}$** are computed from the flux linkage maps and using the following formulae:

$$L_{dq-dynamic} = \frac{\Delta\Phi_d}{\Delta J_q} \qquad L_{qd-dynami} = \frac{\Delta\Phi_q}{\Delta J_d}$$

Note 1: The end-winding leakage inductance Lendw, computed in the winding area, is included in the computation of D-axis and Q-axis flux-linkage. However, the values of the dynamic cross inductances Ldq–dynamic and Lqd-dynamic are not impacted by the end-winding inductance value since they are obtained with the derivative of respectively D-axis and Q-axis flux-linkage with respect to current variation along the corresponding quadrature axis (Q-axis and D-axis respectively).

Note 2: In the previous formulae, one considers peak values for both flux and current.

Note 3: In case the Rotor position dependency is set to "Yes", the computation is done in the J_d - J_q plane with an additional third axis corresponding to the rotor position θ_r.

1.2.5 Static inductances

D-axis synchronous inductance - $L_{d-static}$ and **Q-axis synchronous inductance - $L_{q-static}$** are computed from the flux linkage maps and using the following formulae:

$$L_{d-static} = \frac{(\Phi_d)}{\sqrt{2} \times J_d} \qquad L_{q-static} = \frac{\Phi_q}{\sqrt{2} \times J_q}$$

Note 1: The end-winding leakage inductance L_{endw}, computed in the winding area, is included in the computation of D-axis and Q-axis flux-linkage. The values of the static inductances $L_{d-static}$ and $L_{q-static}$ consider the value of the end-winding inductance.

Note 2: In the previous formulae, one considers peak values for both flux and current.

Note 3: In case the Rotor position dependency is set to "Yes", the computation is done in the J_d - J_q plane with an additional third axis corresponding to the rotor position θ_r.

1.2.6 Saliency

The saliency in Jd-Jq area is computed and displayed as a map in J_d, J_q plane. This value corresponds to the ratio between q-axis and d-axis static inductances.

$$Saliency = \frac{L_{q-static}}{L_{d-stati}}$$

Note: In case the Rotor position dependency is set to "Yes", the computation is done in the J_d - J_q plane with an additional third axis corresponding to the rotor position θ_r.

1.2.7 Electromagnetic torque

The **Electromagnetic torque T_{em}** is computed in different way in function of the input Rotor position dependency value.

1.2.7.1 Rotor position dependency set to “No”

The flux linkage maps and the following formula are used:

$$T_{em} = \frac{m}{2} \times p \times \left(\Phi_d \times J_q - \Phi_q \times J_d\right)$$

Where m is the number of phases (3) and p is the number of pole pairs. J_d and J_q are the d and q axis peak current.

1.2.7.2 Rotor position dependency set to “Yes”

The **Electromagnetic torque T_{em}** is computed thanks to finite element computation and virtual work method to get the best evaluation of the ripple torque.

Note: In case the Rotor position dependency is set to “Yes”, **Electromagnetic torque T_{em}** average value computed with the Park’s equation or with virtual works are equal.

1.2.8 Iron loss computation

The **iron losses** are computed in a different way in the function of the value of the “Rotor position dependency” input.

1.2.8.1 Rotor position dependency set to “No”

A dedicated process has been developed to compute the **stator iron losses** (rotor iron losses not computed).
Stator iron losses are computed only for the stator magnetic circuit built with lamination material (computation is not applicable for solid materials).

Our method of computation doesn’t allow computing iron losses on the rotor side. However, iron loss level is generally not very important on the rotor side in comparison with iron losses on the stator side.

For each node of the grid, in the J_d-J_q space defined and illustrated above, magnetic flux densities in stator teeth are obtained from a dedicated semi-numerical method based on the integration of the flux density in the airgap.

For each considered region (foot teeth, teeth and yoke) we get the magnetic flux density as a function of the angular position. Then, the derivative of each magnetic flux density is computed as a function of the angular position.

At last, for each considered speed, a mathematical transformation is applied to get the derivative of magnetic flux density as a function of time

$$\frac{dB}{dt}(t) = \frac{dB}{d\theta}(\theta) \times \frac{d\theta}{dt}$$

Total iron losses are computed considering the magnetic circuit volume, the density of materials used, and the stacking coefficient considered for the stator lamination.

1.2.8.2 Rotor position dependency set to “Yes”

The **iron losses, stator and rotor** are computed thanks to the magnetostatic application of Flux (Finite Element modeling - MS FE) based on the magnetic flux derivative obtained over the finite element meshing.

The accuracy obtained is the same as the one with a magnetic transient finite element computation (MT FE) and for a given scenario the MS FE computation time is approximately reduced by a factor 2 times lower than MT FE.

1.2.8.3 Model used to compute iron losses

The model used to compute iron losses (W_{iron}) is:

$$W_{iron} = \left[\left(K_h \cdot \left(\frac{B_{max}}{K_f}\right)^{\alpha_h} \cdot f^{\beta_h} \right) + \left(K_c \cdot \frac{1}{T_{elec}} \cdot \int_0^{Telec} \left[\frac{\left(\frac{dB}{dt}\right)}{K_f} \right]^{\alpha_c} dt \right) + \left(K_e \cdot \frac{1}{T_{elec}} \int_0^{Telec} \left[\frac{\left(\frac{dB}{dt}\right)}{K_f} \right]^{\alpha_e} dt \right) \right] . V_{iron} . K_f$$

With:
B_{max}: Peak value of the magnetic flux density (T)
f: Electrical frequency (Hz)
V_{iron}: Stator core lamination volume
K_f: Stacking factor

The other parameters of this model are defined in the application dedicated to materials in FluxMotor®, i.e. “Materials”.

Note: In case the “Rotor position dependency” input is set to “No”, the impact on accuracy will be more important for machine with high level of saturation. In fact, the semi-numerical method used to compute magnetic flux density of the stator teeth neglects flux leakage between teeth. This hypothesis will lead to more errors particularly in areas where there is field weakening (generally applicable at high speeds).

1.2.9 Joule losses

Joule losses in stator winding W_{Cus} are computed using the following formulae:

$$W_{Cus} = m \times R_{ph} \times (J)^2$$

$$\underline{J} = J_d + jJ_q$$

$$|\underline{J}| = J = \sqrt{J_d^2 + J_q^2}$$

Where m is the number of phases (3 in the first version of FluxMotor®),
J is the rms value of the phase current (I is the line current. I = J with a Wye winding connection),
R_{ph} is the phase resistance computed according to the temperatures defined by user in the test settings.

Note 1: R_{ph} considers the resistance factor defined in the winding settings (DESIGN area of Motor Factory).

Note 2: In case the Rotor position dependency is set to “Yes”, the computation is done in the J_d - J_q plane with an additional third axis corresponding to the rotor position θ_r.

1.2.10 Mechanical losses

The mechanical losses are computed as a function of the speed.
For more details, please refer to the document: MotorFactory_2020.2_SMPM_IOR_3PH_Test_Introduction – section “Mechanical loss model settings”

1.2.11 Total losses

For each considered value of speed and currents J_d, J_q, the amount of losses described above (Stator iron loss, Joule loss and mechanical losses) are computed and displayed.

Note: In case the Rotor position dependency is set to “Yes”, the computation is done in the J_d - J_q plane with an additional third axis corresponding to the rotor position θ_r.

2 CHARACTERIZATION – THERMAL – MOTOR & GENERATOR – STEADY STATE

2.1 Overview

2.1.1 Positioning and objective

The aim of “Characterization – Thermal – Motor & Generator – Steady state” test is to evaluate the impact of electromagnetic performance on thermal behavior of the machine.
A thermal working point defined by a speed and a set of losses can be considered to compute the temperature charts and the main thermal parameters. The inputs describing the thermal working point can be set manually or imported from electromagnetic tests that were previously solved.

This test helps to answer the following questions:

- Can the machine operate at the targeted working point without any overheating? Yes / No
- Can the different kinds of proposed cooling help to reach good performance? Yes / No

The following table helps to classify the test “Characterization – Thermal – Motor & Generator – Steady state”.

Family	Characterization
Package	Thermal
Convention	Motor & Generator
Test	Steady state

Positioning of the test “Characterization – Thermal – Motor & Generator – Steady state”.

2.2 Main principles of computation

2.2.1 Introduction

Here are illustrations which give an overview of the thermal test:

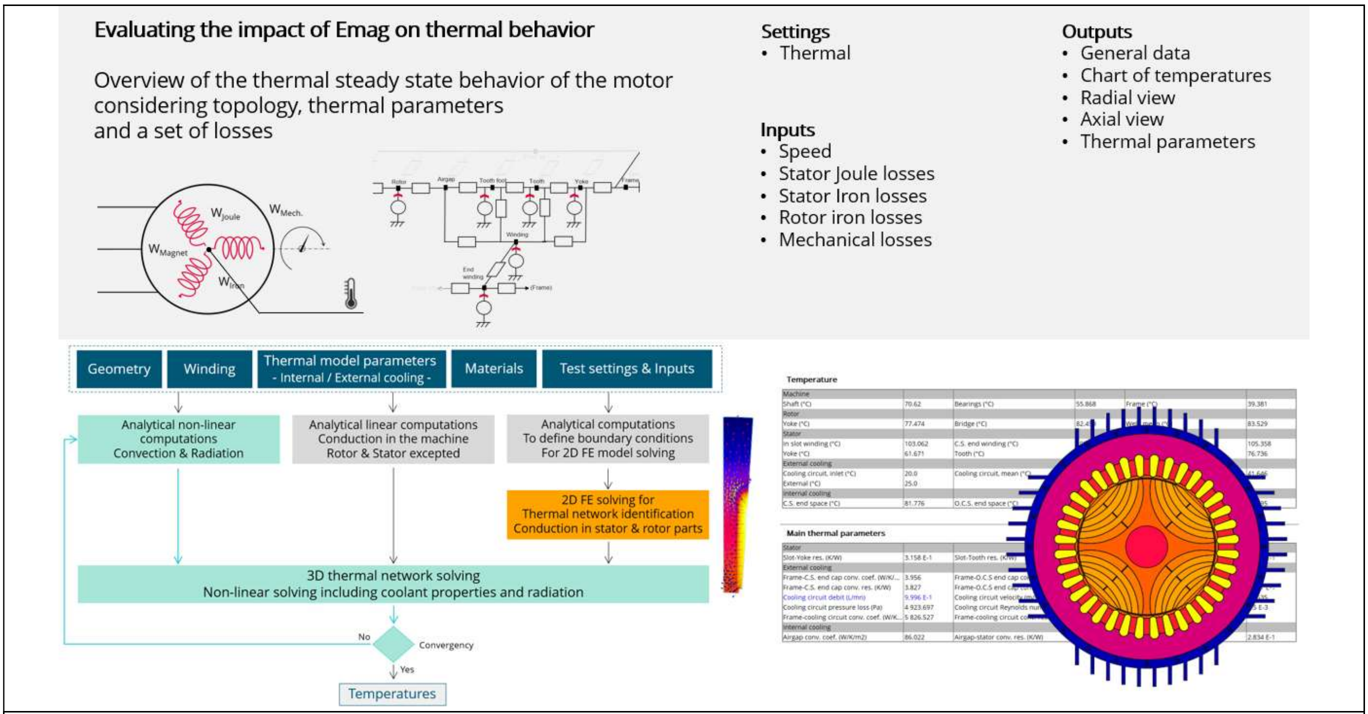

Characterization – Thermal – Steady state – Reluctance Synchronous Machine - Overview

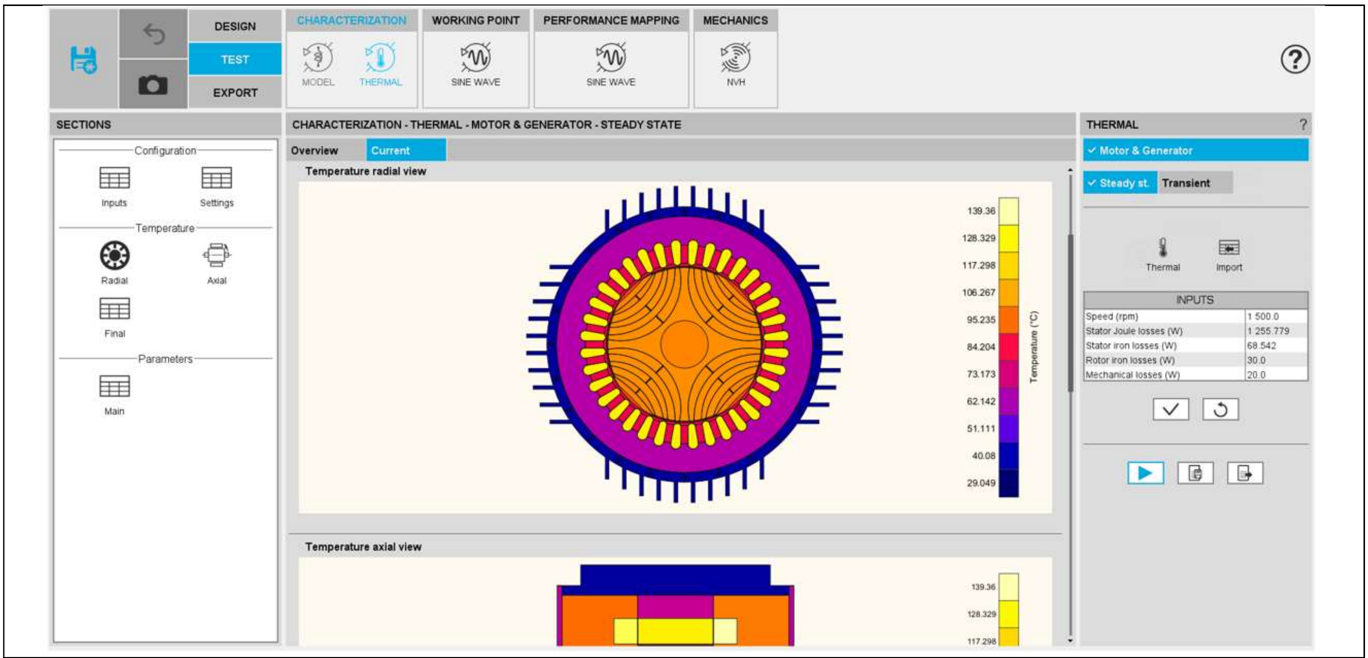

Characterization – Thermal – Steady state – Reluctance Synchronous Machine – Test results

2.2.2 Flow chart

Here is the flowchart illustrating the internal process of the thermal test.

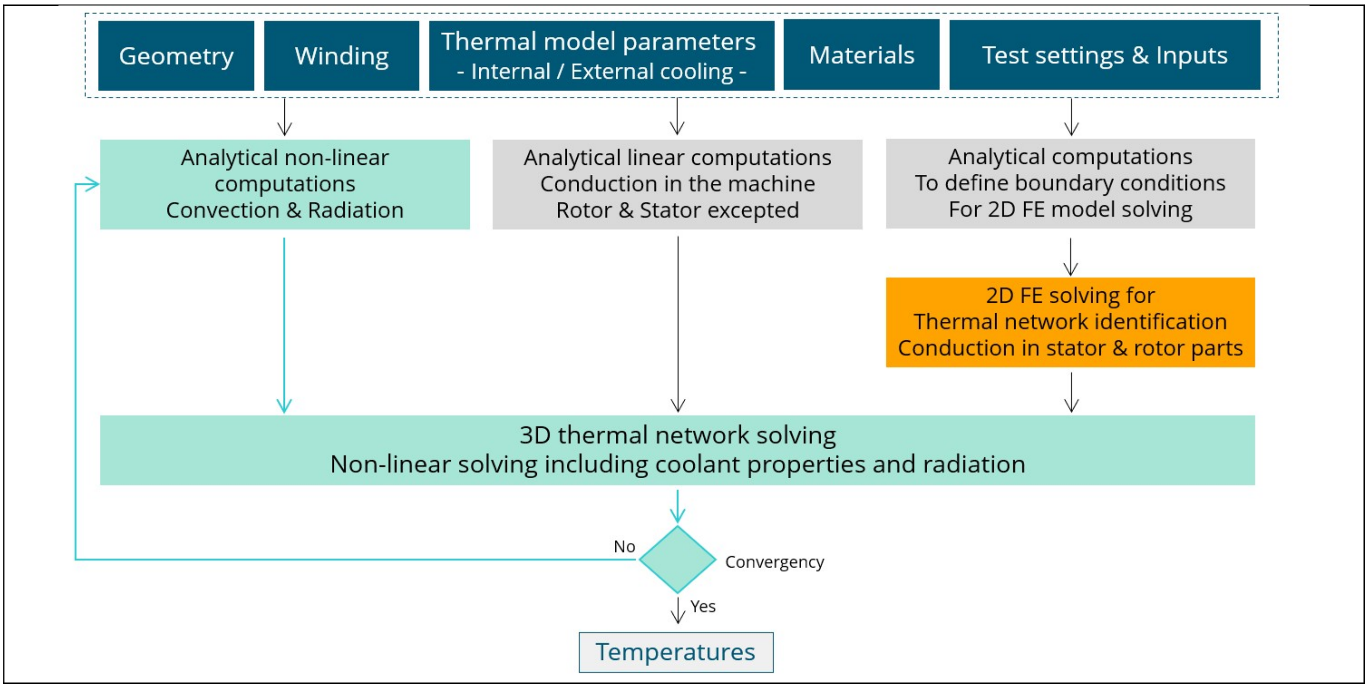

Thermal test – Internal process flowchart

The inputs of the internal process are the parameters of:

- Geometry
- Winding
- Internal cooling
- External cooling
- Materials
- Test settings and inputs

Note: A 2D Finite Element model is solved to identify a thermal network which corresponds accurately to any kind of rotor or stator parts, including user parts.

Then, the resulting network is extended with analytical computations to consider the 3D effect of the geometry.

The solving allows to get and to display the whole chart of temperatures of the machines.

2.3 Limitation of computations - Advice for use

Notes:

1) The resistance network identification of a machine is always done without any skew angle.
This can bring some inaccuracy in the results for highly skewed machines.

2) Please refer to the document: MotorFactory_SMRSM_IR_3PH_Test_Introduction – section “Limitation of thermal computations – Advice for use”

3 CHARACTERIZATION – THERMAL – MOTOR & GENERATOR – TRANSIENT

3.1 Overview

3.1.1 Positioning and objective

The aim of “Characterization – Thermal – Motor & Generator – Transient” test is to evaluate the impact of electromagnetic performance on thermal behavior of the machine in a transient mode.
A thermal working point defined by a speed and a set of losses can be considered to compute the temperature charts and the main thermal parameters. The inputs describing the thermal working point can be set manually or imported from electromagnetic tests that were previously solved.
In addition to that, a maximum evaluation duration and a time step are added as inputs to set the transient mode.

This test helps to answer the following questions:

- Can the machine operate at the targeted working point without any overheating? Yes / No
- Can the different kinds of proposed cooling help to reach good performance? Yes / No
- How long does it take to reach the thermal steady state and what are the thermal time constants of the machine?

The following table helps to classify the test “Characterization – Thermal – Motor & Generator – Steady state”.

Family	Characterization
Package	Thermal
Convention	Motor & Generator
Test	Transient

Positioning of the test “Characterization – Thermal – Motor & Generator – Transient”

3.2 Main principles of computation

3.2.1 Introduction

Here are illustrations which give an overview of the thermal transient test:

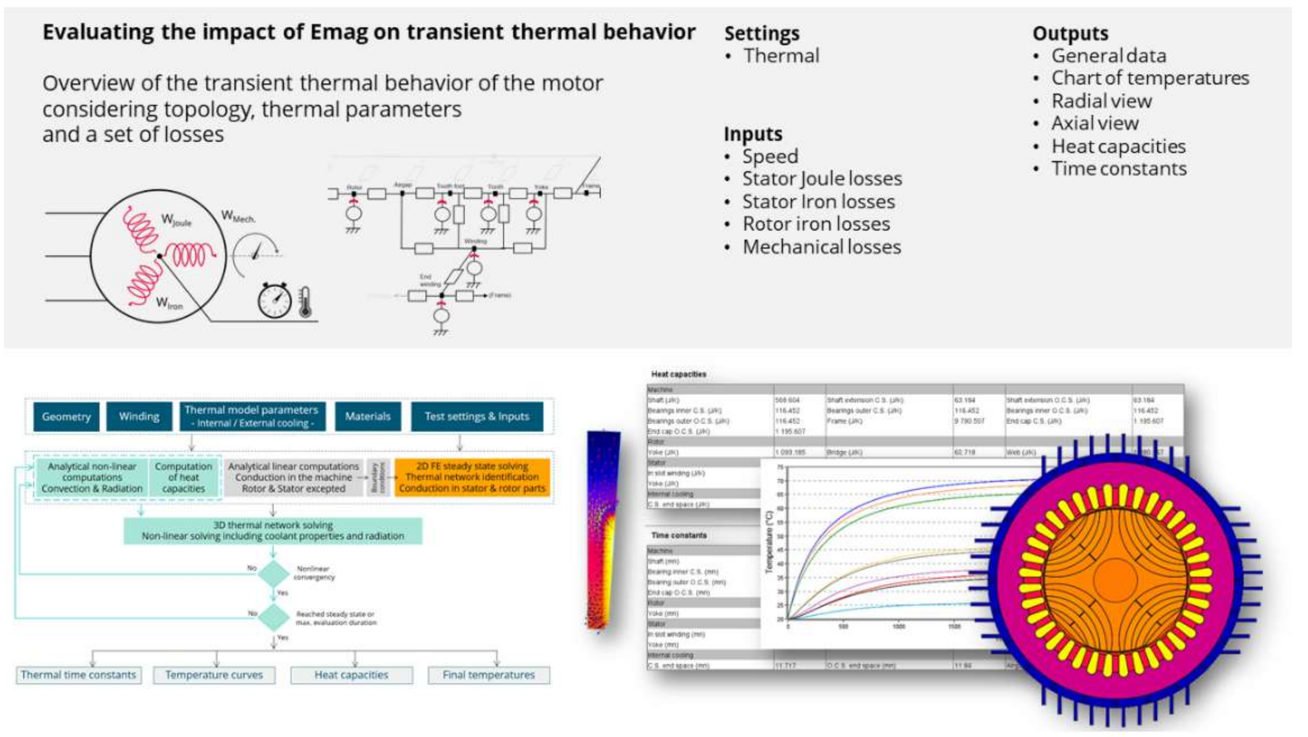

Characterization – Thermal – Transient – Synchronous machine - Overview

Characterization – Thermal – Transient– Synchronous machine – Test results

3.2.2 Flow chart

Here is the flowchart illustrating the internal process of the thermal transient test.

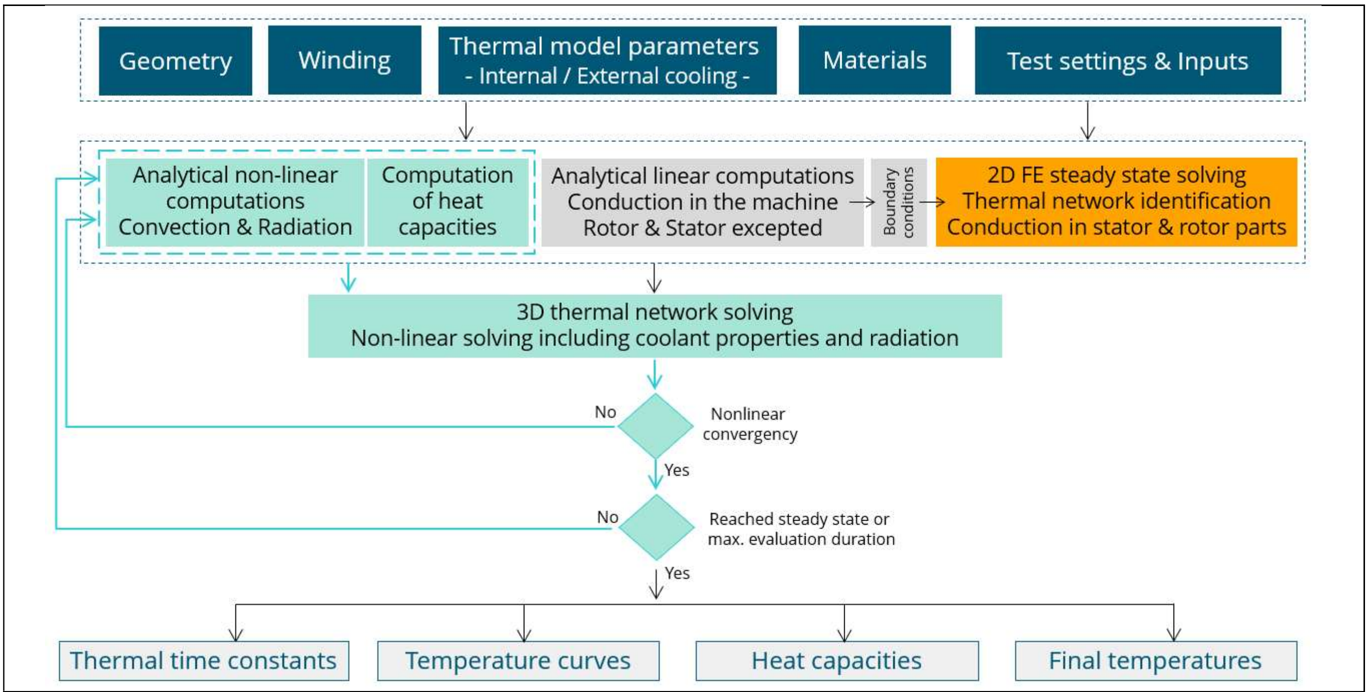

Thermal transient test – Internal process flow chart

The inputs of the internal process are the parameters of:

- Geometry
- Winding
- Internal cooling
- External cooling
- Materials
- Test settings and inputs

A 2D Finite Element model is solved to identify a thermal network which corresponds accurately to any kind of rotor or stator parts, including user parts.
Then, the resulting network is extended with analytical computations to consider the 3D effect of the geometry at each time step. For that, a non-linear computation is performed in the solving of the transient thermal test.
Each thermal node of the machine is associated to a thermal capacitance, depending of the specific heat and density of the material(s) composing the node, and the associated volume.
Thus, the main provided outputs are the whole chart of temperatures of the machines versus time, the heat capacities, and the time constants.

Note: What are the criteria that allow to see if the steady state is reached while thermal transient solving?
First, from the thermal steady state computation, one gets a good estimation of the final temperature (θ_f).
From the thermal transient computation, variation of the temperature versus the time, one deduces the inverse function, i.e. the variation of the time versus the temperature.
Knowing that the time constant to reach 63% of a temperature step is equal to:

$$\theta_\tau = \theta_0 + (1- e^{-1}) \text{ x } (\theta_f - \theta_0).$$

We are looking for the time t that corresponds to θ_τ. If found, it corresponds to tau.
If the evaluation time t considered is lower than τ ($t < \tau$), there is no convergency yet.
If $\tau < t < 5\tau$, there is no convergency, the thermal steady state is not reached yet, but an estimation of time needed to converge can be estimated and given to the user.
If $t > \tau$ The solving has converged, and the steady state is reached.

3.3 Limitation of computations - Advice for use

Notes:

3) The resistance network identification of a machine is always done without any skew angle.
This can bring some inaccuracy in the results for highly skewed machines.

4) Please refer to the document: MotorFactory_SMRSM_IR_3PH_Test_Introduction – section “Limitation of thermal computations – Advice for use”